

# Multiple Differentially Methylated Regions Specific to Keratoconus Explain Known Keratoconus Linkage Loci

Michał Kabza,<sup>1</sup> Justyna A. Karolak,<sup>1,2</sup> Malgorzata Rydzanicz,<sup>3</sup> Monika Udziela,<sup>4</sup> Piotr Gasperowicz,<sup>3</sup> Rafał Płoski,<sup>3</sup> Jacek P. Szaflik,<sup>4</sup> and Marzena Gajecka<sup>1,2</sup>

<sup>1</sup>Department of Genetics and Pharmaceutical Microbiology, Poznan University of Medical Sciences, Poznan, Poland

<sup>2</sup>Institute of Human Genetics, Polish Academy of Sciences, Poznan, Poland

<sup>3</sup>Department of Medical Genetics, Medical University of Warsaw, Warsaw, Poland

<sup>4</sup>Department of Ophthalmology, Medical University of Warsaw, Warsaw, Poland

Correspondence: Marzena Gajecka, Poznan University of Medical Sciences, Department of Genetics and Pharmaceutical Microbiology, Swiecickiego 4, 60-781 Poznan, Poland; gamar@man.poznan.pl.

Submitted: October 9, 2018

Accepted: March 13, 2019

Citation: Kabza M, Karolak JA, Rydzanicz M, et al. Multiple differentially methylated regions specific to keratoconus explain known keratoconus linkage loci. *Invest Ophthalmol Vis Sci.* 2019;60:1501–1509. <https://doi.org/10.1167/iovs.18-25916>

**PURPOSE.** Keratoconus (KTCN) is a complex eye disorder resulting in loss of visual function. Its development is affected by genetic and environmental components. The aim of this study was to unravel the role of epigenetic factors in KTCN.

**METHODS.** To verify if DNA methylation may play a role in KTCN development, reduced representation bisulfite sequencing of five KTCN and five non-KTCN human corneas was performed.

**RESULTS.** Multiple KTCN-specific differentially methylated regions were detected and many of them overlap previously identified KTCN linkage loci (3p14.3, 5q35.2, 13q32.3, 15q24.1, and 20p13) and chromosome arms that have been linked to KTCN (2q, 4q, 5p, 9p, 14q, and 17q). Reanalysis of the previously described RNA sequencing dataset of 25 KTCN and 25 non-KTCN human corneas revealed that 12 genes downregulated in KTCN and 6 upregulated genes overlapped or were located in the near vicinity of the identified differentially methylated regions. Particularly interesting were the DNA methylation changes in *WNT3* and *WNT5A* encoding Wnt ligands, as they provide a potential explanation for the Wnt signaling pathway dysregulation observed in KTCN.

**CONCLUSIONS.** We presented the results of data analysis from the first study of DNA methylation changes in human KTCN corneas compared to non-KTCN samples. We were able to identify genomic regions with distinct patterns of DNA hypo- and hypermethylation and link them to previously found KTCN susceptibility loci as well as transcriptomic disruption of Wnt signaling pathway observed in KTCN.

**Keywords:** keratoconus, human cornea, DNA methylation, RRBS, differentially methylated regions

Keratoconus (KTCN; OMIM 148300) is a degenerative eye disorder characterized by progressive thinning of the cornea, leading to its conical shape and impairment of visual function.<sup>1</sup> The estimated prevalence of KTCN in the general population is between 1 in 2000<sup>1</sup> and 1 in 375 individuals.<sup>2</sup> KTCN is a complex, heterogeneous disease with multifactorial etiology.<sup>3</sup> Its development is affected by environmental and behavioral factors, such as eye rubbing and wearing contact lenses, but also has a strong genetic component indicated by familial inheritance, discordance between dizygotic twins, and association with other known genetic disorders.<sup>4</sup> Multiple loci and gene variants have been linked to KTCN, but they tend to be specific to particular families or populations.<sup>5</sup>

Epigenetic modifications, such as DNA methylation and histone marks, have been suggested to play vital role in shaping complex phenotypes, including disease etiology.<sup>6</sup> These modifications have been shown to be both highly plastic, responding to environmental conditions, and able to alter gene expression in heritable manner.<sup>7</sup> As a result, they offer a potential solution to the problem of “missing heritability,” explaining why identified DNA variants account for only a fraction of observed heritability of many complex traits.<sup>7</sup>

Large-scale epigenetic studies have never been implemented in KTCN research. However, methylation status in KTCN was studied in the *TIMP3* promoter. *TIMP3* encodes tissue inhibitor of metalloproteinase 3 and, due to its overexpression leading to apoptosis in corneal stromal cell, is proposed as one of the candidate genes for KTCN.<sup>8</sup> Methylation-specific quantitative PCR performed in three keratoconic and three healthy corneal tissues excluded promoter methylation in the *TIMP3*, suggesting that factors other than epigenetic factors affect *TIMP3* expression in KTCN.<sup>9</sup>

Herein, we present the results of a DNA methylation study performed in human corneas derived from five KTCN and five non-KTCN individuals by using reduced representation bisulfite sequencing (RRBS).<sup>10</sup> We were able to identify multiple regions that show distinct patterns of DNA hypo- and hypermethylation in KTCN. The majority of these differentially methylated regions (DMRs) were located within annotated gene bodies, including genes coding for two Wnt ligands that we previously discussed in the context of KTCN.<sup>11</sup> We also found that many of detected DMRs overlap previously described KTCN susceptibility regions.<sup>5</sup>



## METHODS

### Patients

All individuals underwent a complete ophthalmic evaluation in the Department of Ophthalmology, Medical University of Warsaw, Poland. The detailed ascertainment and examination processes in KTCN patients have been previously described.<sup>11,12</sup> Briefly, the diagnosis of KTCN was based on both corneal topography and pachymetry assessment, a best-corrected visual acuity testing, and a slit-lamp examination. Patients were considered as having KTCN if they had at least one clinical sign, including corneal thinning, Vogt's striae, or Fleischer rings in slit-lamp biomicroscopy concurrent with the changes in topography and pachymetry assessment (Supplementary Table S1).

The study protocol was approved by the Institutional Review Board at Poznan University of Medical Sciences. All individuals provided informed consent after the possible consequences of the study were explained, in accordance with the Declaration of Helsinki.

### Material Collection and DNA Extraction

The corneal tissues were obtained from five KTCN patients and five non-KTCN individuals undergoing a penetrating keratoplasty procedure. The non-KTCN corneas, used as controls, were collected from patients who were referred for corneal transplantation for reasons other than KTCN, including bullous keratopathy, corneal scarring, and perforations (Supplementary Table S1). The corneas were preserved in the Eusol-C solution (Alchimia, Ponte San Nicolo PD, Italy) directly after corneal button excision during the surgical procedure, and stored at 4°C until DNA extraction. Genomic DNA samples from the corneas were extracted using the Cells and Tissue DNA Isolation Kit (Norgen Biotek, Thorold, ON, Canada) according to the manufacturer's protocol.

### RRBS Library Preparation and Sequencing

RRBS libraries were performed using the NEXTflex Bisulfite Library Preparation Kit (Bioo Scientific, Austin, TX, USA) according to manufacturer's instructions. In brief, 500 ng of high-molecular-weight genomic DNA was used for *MspI* digestion (New England Biolabs, Ipswich, MA, USA) followed by DNA purification using Agencourt AMPure XP magnetic beads (Beckman Coulter, Beverly, MA, USA). Purified fragmented DNA samples with 5'-CG-3' overhangs were subject into end repair, adenylation, and adaptor ligation reactions. Bisulfite conversion was performed using the EZ DNA Lightning Kit (Zymo Research, Irvine, CA, USA), according to the manufacturer's instructions, and it was followed by PCR amplification. The PCR products were purified using Agencourt AMPure XP magnetic beads (Beckman Coulter). Prior to sequencing, RRBS libraries were quantified using Qubit instrument (ThermoFisher Scientific, San Jose, CA, USA) and qualified using Agilent 2100 Bioanalyzer High Sensitivity chips (Agilent Technologies, Santa Clara, CA, USA). Paired-end sequencing (2 × 100 bp) was performed on the HiSeq 1500 platform (Illumina, Scientific, San Diego, CA, USA).

### RRBS Data Analysis

Illumina adapters and poor-quality regions (mean Phred quality, <5) were trimmed from short reads by using the BBDuk2 program from the BBTools suite (<http://jgi.doe.gov/data-and-tools/bbtools/>). Bismark<sup>13</sup> was used to align filtered read pairs to the human reference genome (GRCh38) and

calculate DNA methylation percentage at each CpG site. The first five bases from the 5' end of all reads were excluded from methylation calling based on the methylation bias observed in the M-bias plots from Bismark reports. The methylKit package was used to create sample correlation and principal component analysis (PCA) plots (Supplementary Figs. S1 and S2).<sup>14</sup> The DSS package<sup>15</sup> was used to detect DMRs between KTCN and non-KTCN samples by using recommended settings for RRBS experiments. The DSS package performs individual differential methylation tests for each CpG-context cytosine and merges the adjacent significant results (<50 bp distance, minimum 3 CpGs, and minimum 10 percentage point difference in methylation) into DMRs. The raw *P* value threshold of 0.001 was selected, as suggested by DSS documentation for RRBS experiments. BEDTools<sup>16</sup> was used to find the closest gene for each identified DMR. The karyotype plot showing found DMRs and KTCN susceptibility loci (Fig. 1) was created using the karyoplotER package.<sup>17</sup> KTCN linkage loci overlapped by DMRs were visualized (Fig. 2) using the Gviz package.<sup>18</sup> The plot showing the overlap between DMRs and different types of annotated genomic features (Supplementary Fig. S3) was prepared using the ChIPseeker package.<sup>19</sup>

### RNA Sequencing (RNA-Seq) Data Reanalysis

To compare the results of the differential methylation analysis with changes on the transcriptome level, the previously described RNA-Seq dataset of 25 KTCN and 25 non-KTCN human corneas was used.<sup>11</sup> Adapter trimming and poor-quality region removal were performed in the identical way to the RRBS data analysis. Short reads matching human rRNA sequences were additionally removed using BBDuk2. Salmon<sup>20</sup> was used to estimate the expression values for genes and transcripts from GENCODE 25 (Ensembl 87) annotations while accounting for sequence-specific and GC content bias. Differential expression analysis was performed using a previously published protocol<sup>21</sup> using the limma package.<sup>22</sup> Genes were determined to be differentially expressed based on the 0.01 false discovery rate threshold value and 1.5-fold change cutoff.

## RESULTS

All of the analyzed samples had a similar number of cytosines covered by at least 10 reads (2–3 million). Based on the methylation percentage of 457,621 sites that had this coverage in all samples, sample correlation plot (Supplementary Fig. S1) and sample PCA plot (Supplementary Fig. S2) were prepared.

Overall, 112 DMRs between KTCN and non-KTCN samples were detected. Of these, 43 regions were hypermethylated in KTCN corneas, while 69 showed signs of hypomethylation (Fig. 1). Seven DMRs (Fig. 2) overlapped known KTCN linkage loci, namely, 3p14.3,<sup>23</sup> 5q35.2,<sup>24</sup> 13q32.3,<sup>25</sup> 15q24.1,<sup>26</sup> and 20p13,<sup>27</sup> whereas 15 DMRs were located on six chromosome arms, namely, 2q, 4q, 5p, 9p, 14q, and 17q, that have been linked to KTCN.<sup>5,28</sup> The detailed information regarding each region is presented in the Table. None of the identified DMR regions overlapped known genome-wide association study loci.<sup>29–35</sup>

The majority of DMRs (65%, 73 regions) overlapped known genes (the detailed overlap status between DMRs and different categories of genomic annotations is presented in Supplementary Fig. S3). For the remaining 39 regions, the nearest annotated gene was located within a distance between 93 bp and over 360 kb (Table). The comparison of the set of DMR-related genes with the results of differential expression analysis (Supplementary Table S2) based on the previously described corneal RNA-Seq data<sup>11</sup> showed that 18 genes were common to

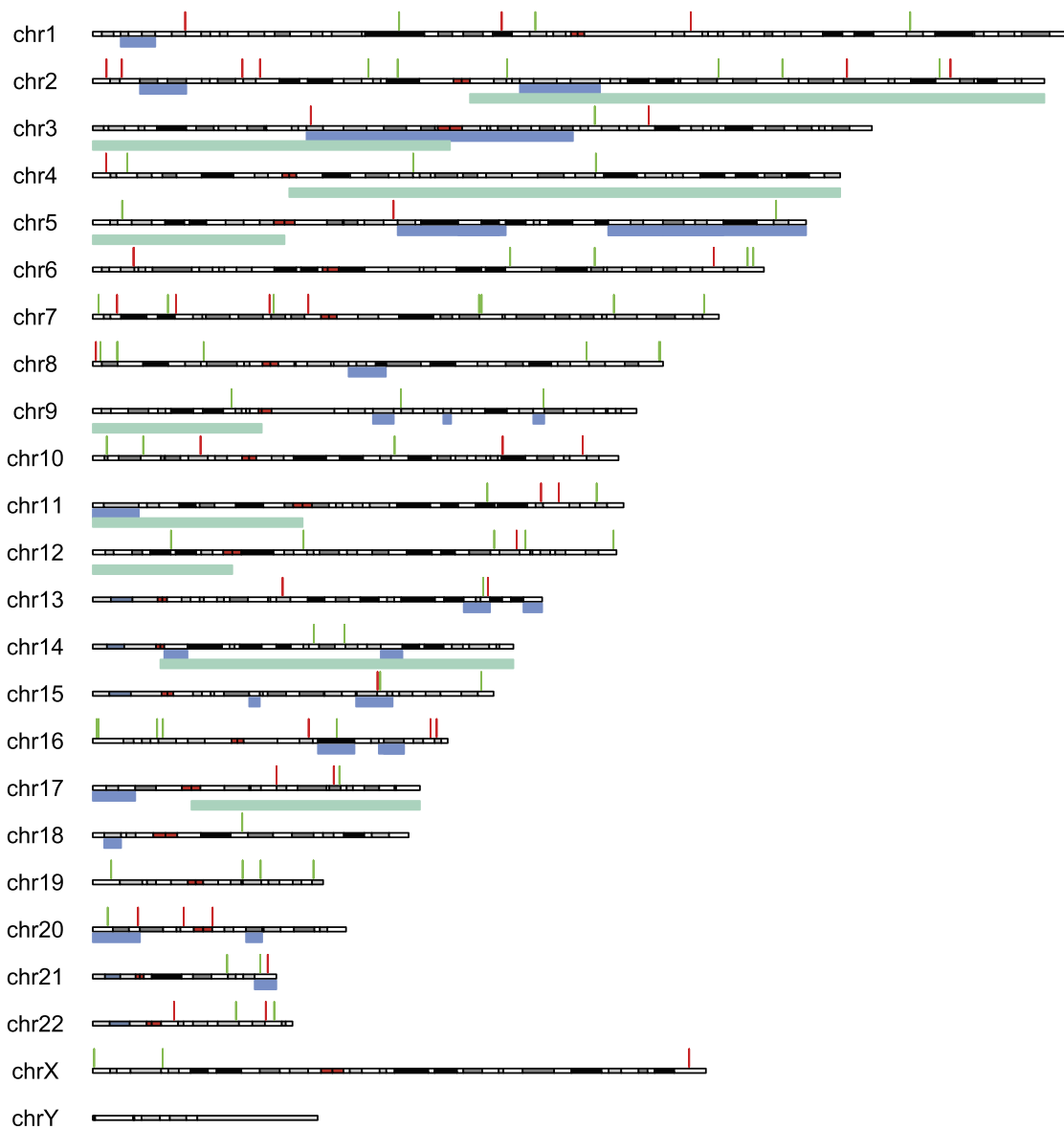


**FIGURE 1.** Differential methylation regions (DMRs) between KTCN and non-KTCN samples. The karyotype plot shows hypermethylated (*red*) and hypomethylated (*green*) DMRs located on each chromosome (centromeres are colored *red*). KTCN linkage regions (*blue*) and chromosomal arms linked to KTCN (*aquamarine*) are shown below chromosomes and were taken from a paper by Karolak and Gajecka.<sup>5</sup>

both datasets. Among the genes overlapping recognized DMRs, 12 genes (*IQGAP2*, *SYNJ2*, *CYP11B1*, *MYO1G*, *WNT5A*, *PARVB*, *MGLL*, *CDC25B*, *PSG3*, *FHL2*, *CAMK1D*, and *THEMIS*) showed downregulated expression in KTCN corneas, whereas 6 genes (*WNT3*, *RBI*, *AC098617.1*, *RPS6KA2*, *PELI2*, and *PLXNA4*) were upregulated in KTCN tissues (Table).

## DISCUSSION

Despite many years of research, the genetic factors responsible for the development of KTCN remain elusive. A number of genomic regions and sequence variants have been associated with KTCN but turned out to be specific to particular families or populations and failed to explain the cause of the disease in the general population.<sup>5</sup> A potential solution to this problem of missing heritability has been recently suggested, as epigenetic modifications, including DNA methylation and histone modifications, were shown to affect phenotype in heritable

manner.<sup>6,7</sup> To verify if this is the case for KTCN, we performed the comprehensive analysis of DNA methylation in human KTCN and non-KTCN corneas using the RRBS approach.<sup>10</sup>

Large-scale epigenetic studies have never been implemented in KTCN research. However, methylation status in KTCN was studied in *TIMP3* promoter. *TIMP3* encodes tissue inhibitor of metalloproteinase 3 and due to its overexpression leading to apoptosis in corneal stromal cell is proposed as one of the candidate genes for KTCN. Methylation-specific quantitative PCR performed in three keratoconic and three healthy corneal tissues excluded promoter methylation in the *TIMP3*, suggesting that other than epigenetic factors affect *TIMP3* expression in KTCN.

In this study, RRBS was used to analyze DNA methylation in human corneas from five KTCN and five non-KTCN individuals. We identified 112 DMRs with distinct patterns of DNA hypermethylation (43 regions) or hypomethylation (69 regions) in KTCN and assigned the nearest gene to each locus. Interestingly, the majority (65%) of the DMRs were located

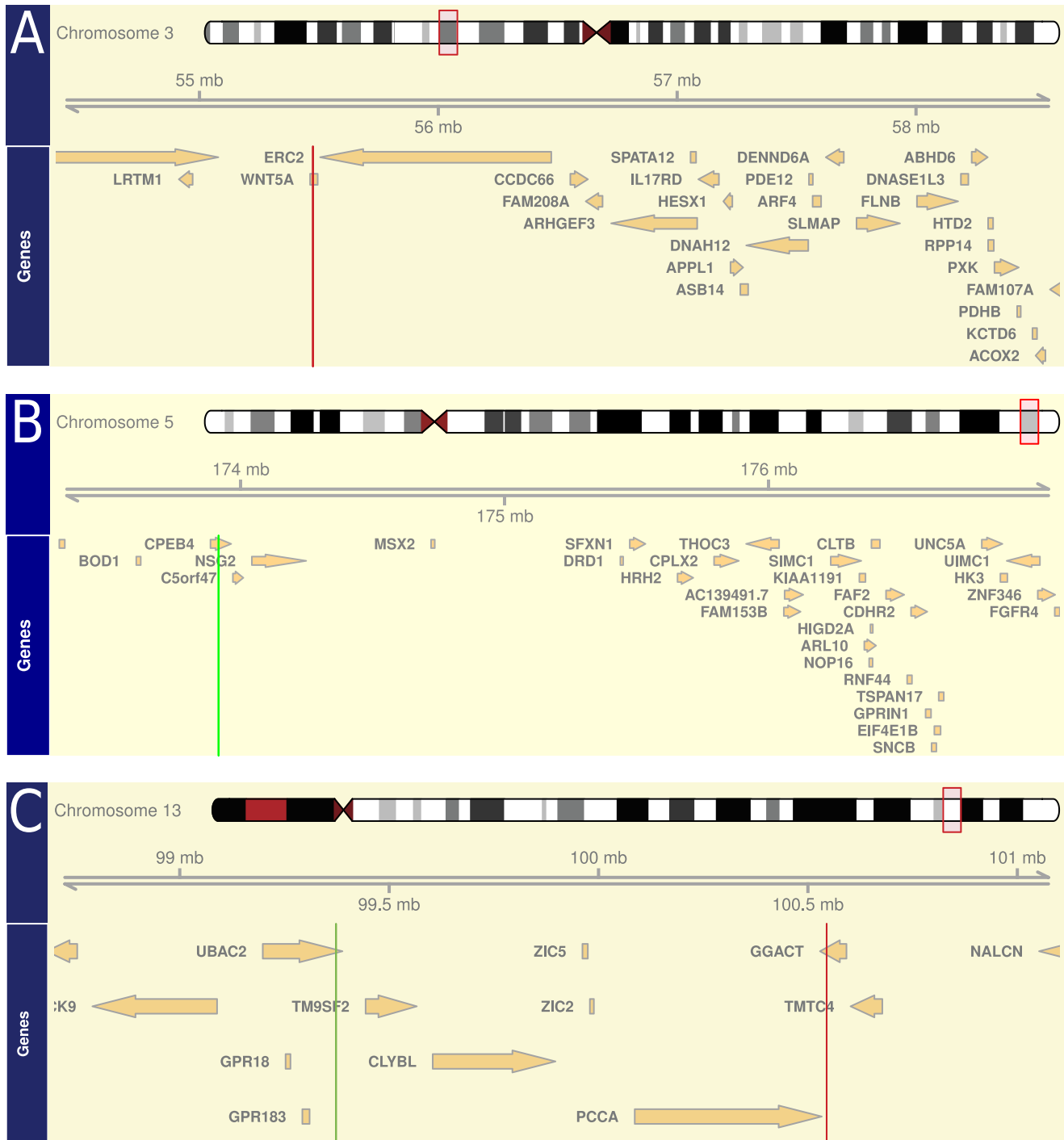


**FIGURE 2.** KTCN linkage loci overlapped by differential methylation regions (DMRs). The plots show the detailed view of the KTCN linkage loci 3p14.3 (A), 5q35.2 (B), 13q32.3 (C), 15q24.1 (D), and 20p13 (E) overlapped by DMRs. Hypermethylated and hypomethylated DMRs are colored *red* and *green*, respectively. Only protein-coding genes are shown.

within annotated gene bodies and not in the intergenic space, as it would be expected for regulatory regions (e.g., promoters) commonly associated with CpG islands studied in RRBS experiments. Many of the identified DMRs overlapped previously described KTCN susceptibility loci. Seven DMRs were located on the known KTCN linkage regions 3p14.3,<sup>23</sup> 5q35.2,<sup>24</sup> 13q32.3,<sup>25</sup> 15q24.1,<sup>26</sup> and 20p13,<sup>27</sup> which further verifies the previously described linkage between these chromosomal loci and KTCN. Moreover, 15 DMRs were located

on the six chromosome arms 2q, 4q, 5p, 9p, 14q, and 17q, previously reported as possibly linked to KTCN.<sup>5,28</sup> These linkage regions contain hundreds of genes and our analysis may allow for significant narrowing of the genomic region of interest and reduce the list of putative KTCN genes from these chromosome arms. None of the identified DMRs region overlapped known genome-wide association study loci, including *HGF*, *RAB3GAP1*, *LOX*, *RXRA-COL5A1*, *MPDZ-NF1B*, and *BANP-ZNF469*.<sup>29-35</sup>



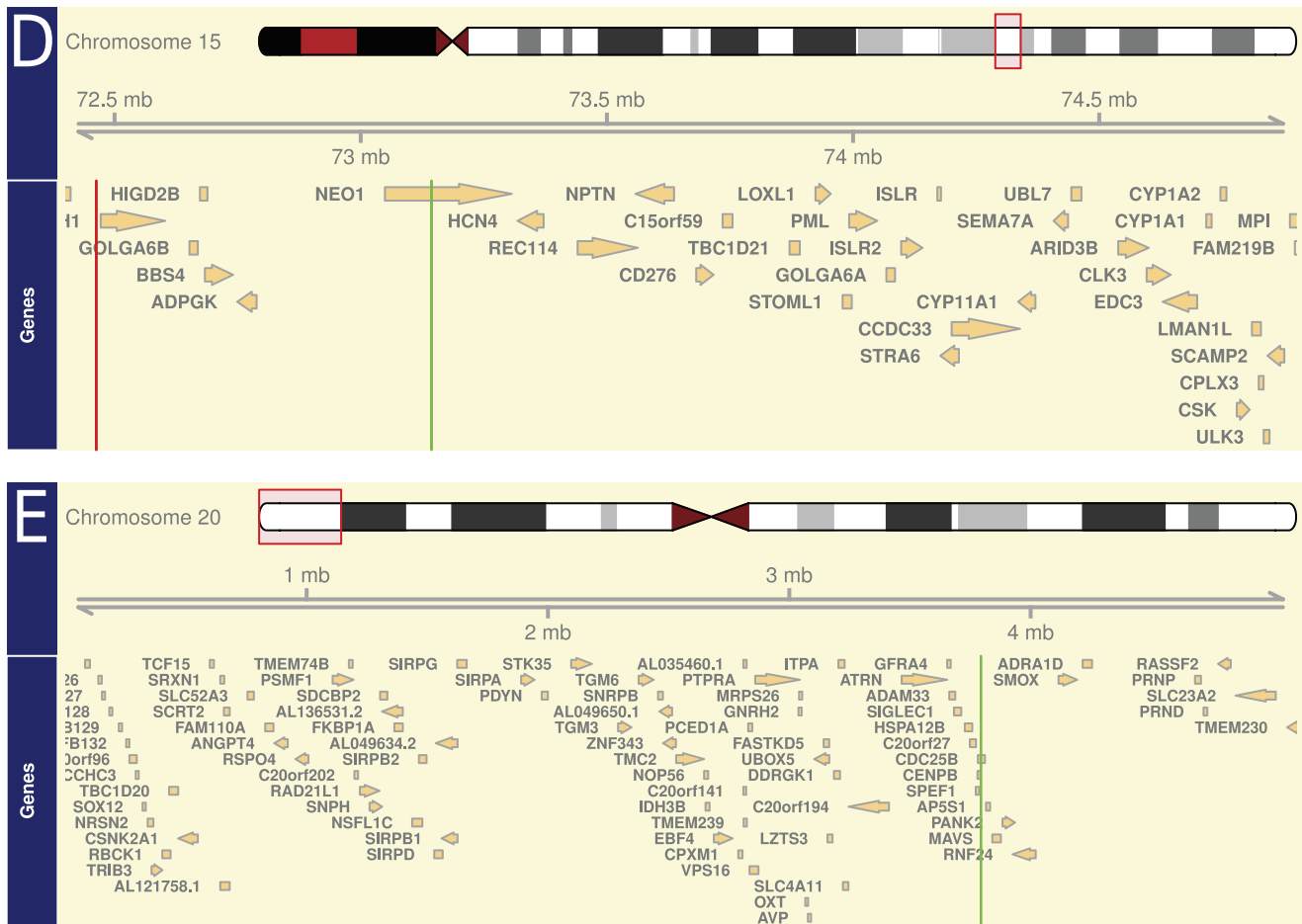


FIGURE 2. Continued.

The next step was comparing the RRBS results with reanalyzed data from the published RNA-Seq study previously performed in human KTCN and non-KTCN corneas. The most interesting finding was that two DMRs located on chr3:55,474,327-55,474,562 and chr17:46,769,843-46,769,996 overlapped the exons of Wnt family member genes *WNT5A* and *WNT3*, respectively. These genes encode important ligands of the Wnt signaling pathway that was previously found to be downregulated in KTCN corneas.<sup>11</sup> Wnt signaling is involved in regulating the proliferation of corneal epithelial stem cells,<sup>36</sup> which suggests that the dysregulation of genes involved in this biological pathway is not incidental and may play a role in KTCN development. Moreover, the first DMR located on chr3:55,474,327-55,474,562 also overlaps the 3p14-q13 KTCN susceptibility locus detected by linkage analysis in an Italian family.<sup>23</sup> *COL8A1* has been first suggested as candidate gene located within this locus, but no pathogenic variants of *COL8A1* have been found in KTCN patients.<sup>23,37</sup> On the other hand, the second region chr17:46,769,843-46,769,996 is located on the 17q chromosome arm that shows linkage to KTCN in the Hispanic population.<sup>30</sup>

Although both regions are hypermethylated in KTCN, *WNT5A* is transcriptionally downregulated, whereas *WNT3* is transcriptionally upregulated in KTCN corneas.<sup>11</sup> This discrepancy can be explained by the fact that DNA methylation of the gene body can affect alternative splicing and indirectly gene expression by using multiple different mechanisms.<sup>38</sup>

Other differentially expressed genes overlapping or located in the near vicinity of the DMRs include *IQGAP2*, *SYNJ2*,

*CYP1B1*, *MYO1G*, *PARVB*, *MGLL*, *CDC25B*, *PSG3*, *FHL2*, *CAMK1D*, *THEMIS* (downregulated), *RB1*, *AC098617.1*, *RPS6KA2*, *PELI*, and *PLXNA4* (upregulated).

Apart from providing some explanation behind the transcriptomic changes observed in KTCN, DNA methylation can also be potentially linked to other important KTCN-related phenomena. Increased levels of interleukin-6 and tumor necrosis factor- $\alpha$  have been repeatedly found in the tears of KTCN patients.<sup>39</sup> Their levels in the tear fluid are also increased by eye rubbing, a known KTCN risk factor.<sup>39</sup> Both proteins have also been shown to be able to induce changes in DNA methylation that affect gene expression.<sup>40,41</sup> In this way, DNA methylation provides us with the unified framework linking hereditary and environmental factors with transcriptomic and phenotypic effects specific to KTCN.

There was high heterogeneity of the control group used in this study, as it was not possible to obtain “healthy” corneas from living individuals for comparative analyses. The small sample size disabled a reliable statistical analysis, and due to this limitation, the general conclusions could not be made. Additionally, the lower sample correlation (Supplementary Fig. S1) and higher sample variability on PCA plot (Supplementary Fig. S2) observed in KTCN samples may suggest that the methylation dysregulation in KTCN results in biological heterogeneity exceeding that of the control group. However, the results of this pilot study have given an additional insight into the role of methylation in KTCN development and showed the possible indications for further KTCN research.

TABLE. A List of Annotated Differential Methylation Regions Detected in This Study

Chromosome	Start	End	Number of CGs	Mean Methylation KTCN, %	Mean Methylation Non-KTCN, %	Diff Methylation, %	Band	Distance, bp	Gene Symbol
5	76543172	76543244	4	96.33	12.2	84.13	5q13.3	0	<i>IQGAP2</i> ↓
2	218297795	218297870	4	90.58	7.73	82.84	2q35*	0	<i>PNKD</i>
6	158040790	158040885	4	95.47	12.99	82.48	6q25.3	0	<i>SYNJ2</i> ↓
10	27413626	27413698	6	90.58	9.59	80.99	10p12.1	0	<i>PTCHD3</i>
2	38073740	38073815	7	93.42	13.99	79.43	2p22.2	0	<i>CYP11B1</i> ↓
4	3373177	3373266	12	92.55	13.3	79.24	4p16.3	0	<i>RGS12</i>
11	114082993	114083071	9	91.47	12.92	78.54	11q23.2	0	<i>ZBTB16</i>
20	30485824	30485883	8	94.39	17.33	77.06	20q11.21	-749	<i>5_Ss_rRNA</i>
7	44979190	44979242	5	85.75	10.13	75.62	7p13	-93	<i>MYO1G</i> ↓
3	55474327	55474562	51	83.62	9.9	73.72	3p14.3†	0	<i>WNT5A</i> ↓
21	44504301	44504403	9	88.36	14.87	73.49	21q22.3	0	<i>TSPEAR</i>
6	10390769	10390836	7	83.96	11.02	72.95	6p24.3	2,350	<i>TFAP2A</i>
15	72462249	72462347	4	81.18	9.66	71.52	15q24.1†	0	<i>RP11-1007024.3</i>
6	10385681	10385732	5	88.63	17.23	71.4	6p24.3	7,454	<i>TFAP2A</i>
10	104326111	104326301	8	89.66	18.28	71.38	10q25.1	0	<i>ITPRIP</i>
22	44027177	44027235	5	91.84	20.48	71.36	22q13.31	0	<i>PARVB</i> ↓
7	54833167	54833263	19	89.95	22.13	67.83	7p11.2	28,240	<i>RP11-745C15.2</i>
10	124677537	124677608	8	91.65	25.08	66.58	10q26.13	0	<i>RP11-12J10.3</i>
2	3483393	3483453	5	83.17	16.91	66.25	2p25.3	0	<i>TRAPPC12</i>
2	7378775	7378859	5	89.94	24.97	64.97	2p25.1	-42,402	<i>AC013460.1</i>
22	20671140	20671193	6	78.17	14.28	63.89	22q11.21	-157	<i>ABHD17AP4</i>
13	100544955	100545129	18	89.11	26.06	63.05	13q32.3†	0	<i>GGACT</i>
16	54938843	54938915	18	90.67	27.95	62.71	16q12.2	0	<i>CTD-3032H12.2</i>
20	23157733	23157831	15	72.24	10.93	61.31	20p11.21	3,026	<i>RNA5SP478</i>
16	85948241	85948359	20	92.57	32.19	60.37	16q24.1	-12,019	<i>RP11-542M13.3</i>
11	118609670	118609752	18	87.27	27.18	60.09	11q23.3	0	<i>PHLDB1</i>
7	54833322	54833422	25	82.38	23.45	58.92	7p11.2	28,395	<i>RP11-745C15.2</i>
2	42547287	42547366	5	81.99	23.86	58.13	2p21	0	<i>MTA3</i>
7	21169179	21169304	6	78.19	20.6	57.59	7p15.3	46,233	<i>RN7SL542P</i>
12	107864368	107864418	9	78.69	22.03	56.66	12q23.3	0	<i>RP11-554D14.6</i>
7	6170857	6170975	23	82.46	26.51	55.95	7p22.1	0	<i>CYTH3</i>
17	46769843	46769996	37	88.63	33.55	55.08	17q21.32*	0	<i>WNT3</i> ↑
1	152188864	152188973	13	78.37	23.54	54.83	1q21.3	0	<i>PUDPP2</i>
16	87516095	87516166	4	95.72	41.74	53.98	16q24.2	461	<i>RP11-482M8.1</i>
8	789263	789335	7	95.94	41.97	53.97	8p23.3	0	<i>DLGAP2</i>
13	48318907	48318957	11	67.19	13.65	53.54	13q14.2	0	<i>RBI</i> ↑
17	61313850	61313902	7	74.32	24.44	49.88	17q23.2*	0	<i>BCAS3</i>
1	104073014	104073082	13	90.99	41.38	49.61	1p21.1	0	<i>RP11-364B6.2</i>
X	151776566	151776673	7	88.65	41.7	46.95	Xq28	31,263	<i>CNGA2</i>
2	191953921	191953975	9	90.83	47.01	43.82	2q32.3*	0	<i>AC098617.1</i> ↑
1	23503550	23503637	9	85.21	43.38	41.82	1p36.12	2793	<i>E2F2</i>
3	141483864	141483918	5	77.21	39.6	37.61	3q23	-3,129	<i>RASA2</i>
20	11513917	11513973	13	76.11	44.37	31.74	20p12.2	22,433	<i>RP5-1128N12.3</i>
8	6352375	6352438	5	29.91	67.91	-38	8p23.1	51,113	<i>RP11-115C21.2</i>
22	46176937	46176993	7	50.84	90.74	-39.9	22q13.31	0	<i>PPARA</i>
7	19124849	19124910	9	45.94	87.26	-41.32	7p21.1	2,934	<i>AC003986.7</i>
X	344575	344649	7	47.29	93.66	-46.37	Xp22.33	0	<i>PPP2R3B</i>
4	128047509	128047582	13	45.89	94.51	-48.62	4q28.2*	7,799	<i>ABHD18</i>
3	127757772	127757824	5	44.71	93.66	-48.96	3q21.3	0	<i>MGLL</i> ↓
7	1470564	1470646	11	45.38	94.58	-49.19	7p22.3	0	<i>INTS1</i>
8	28210681	28210759	5	42.46	91.88	-49.42	8p21.1	-15,170	<i>RP11-380I10.2</i>
6	166652695	166652750	5	44.58	95.51	-50.94	6q27	0	<i>RPS6KA2</i> ↑
9	35297277	35297331	5	41.37	92.96	-51.6	9p13.3*	0	<i>UNC13B</i>
10	3552153	3552211	5	39.63	91.36	-51.73	10p15.2	-15,123	<i>RP11-482E14.2</i>
20	3794919	3794972	5	39.78	92	-52.22	20p13†	0	<i>CDC25B</i> ↓
12	132522093	132522166	7	28.57	84.09	-55.52	12q24.33	0	<i>FBRSL1</i>
4	8784319	8784372	5	8.63	66.27	-57.64	4p16.1	-38,287	<i>RP11-1338A24.1</i>
2	159246171	159246229	5	10.35	69.09	-58.73	2q24.2*	0	<i>WDSUB1</i>
16	1465186	1465247	9	26.01	86.44	-60.43	16p13.3	0	<i>CLCN7</i>
17	62759716	62759766	4	9.67	72.52	-62.85	17q23.2*	0	<i>MARCH10</i>
16	975463	975522	5	28.06	92.52	-64.46	16p13.3	0	<i>LMF1</i>

TABLE. Continued

Chromosome	Start	End	Number of CGs	Mean Methylation KTCN, %	Mean Methylation Non-KTCN, %	Diff Methylation, %	Band	Distance, bp	Gene Symbol
9	78410193	78410246	5	27.1	93.65	-66.55	9q21.2	80,101	<i>PSAT1</i>
15	98865943	98866006	7	13.39	80.57	-67.18	15q26.3	0	<i>IGF1R</i>
7	98948567	98948618	4	28.34	95.6	-67.26	7q22.1	0	<i>TRRAP</i>
7	98303586	98303639	5	24.06	93.72	-69.66	7q21.3	0	<i>BRI3</i>
2	77593138	77593188	5	22.31	93.18	-70.86	2p12	0	<i>LRRTM4</i>
12	53615315	53615370	4	10.17	81.85	-71.68	12q13.13	0	<i>RP11-793H13.10</i>
11	100409101	100409233	10	15.12	86.99	-71.88	11q22.1	50,217	<i>CNTN5</i>
16	17839567	17839632	4	14.53	86.46	-71.93	16p12.3	12,662	<i>CTD-3229J4.1</i>
6	168095867	168095941	6	22.42	95	-72.58	6q27	-14,311	<i>FRMD1</i>
18	38033855	38033982	7	10.6	83.3	-72.7	18q12.2	360,680	<i>RPL12P40</i>
19	42698055	42698145	9	9.68	82.51	-72.83	19q13.2	23,493	<b>PSG3</b> ↓
14	56290295	56290361	5	11.98	85.93	-73.95	<b>14q22.3*</b>	0	<b>PELI2</b> ↑
1	208043110	208043184	5	13.94	87.98	-74.04	1q32.2	0	<i>PLXNA2</i>
12	19903560	19903621	5	21.21	95.85	-74.64	12p12.3	0	<i>RP11-405A12.2</i>
19	4675865	4675921	5	12.7	87.53	-74.83	19p13.3	0	<i>DPP9</i>
16	62114488	62114563	5	12.6	88.16	-75.56	16q21	72,977	<i>RNU6-21P</i>
2	215545625	215545688	8	11.24	87.1	-75.86	<b>2q35*</b>	0	<i>AC012668.2</i>
8	1931560	1931639	7	17	92.91	-75.91	8p23.3	0	<i>RP11-439C15.6</i>
12	110114235	110114353	4	17.72	93.99	-76.27	12q24.11	-9,982	<i>IFT81</i>
7	155577505	155577589	4	8.6	86.42	-77.82	7q36.3	0	<i>RP5-912I13.2</i>
8	144109249	144109310	4	9.3	87.71	-78.41	8q24.3	0	<i>WDR97</i>
5	173914687	173914781	5	8.54	87.23	-78.69	<b>5q35.2†</b>	0	<i>CPEB4</i>
19	56159826	56159907	12	13.44	92.42	-78.98	19q13.43	0	<i>ZNF444</i>
1	112631642	112631693	4	14.95	93.94	-78.99	1p13.2	0	<i>CAPZA1</i>
8	144426833	144426889	4	12.48	91.7	-79.23	8q24.3	0	<i>VPS28</i>
14	64038589	64038661	7	15.86	95.48	-79.63	<b>14q23.2*</b>	0	<i>SYNE2</i>
10	76815006	76815078	4	9.9	90.09	-80.2	10q22.3	20,299	<i>SNORA31</i>
22	36439313	36439377	4	11.22	91.85	-80.63	22q12.3	1,503	<i>Y_RNA</i>
7	132619824	132619887	4	13.5	94.66	-81.16	7q32.3	0	<b>PLXNA4</b> ↑
2	70169790	70169908	4	10.62	91.85	-81.23	2p13.3	0	<i>C2orf42</i>
15	73143464	73143527	5	12.77	94.21	-81.45	<b>15q24.1†</b>	0	<i>NEO1</i>
9	114683367	114683443	4	11.67	93.19	-81.52	9q32	-1,302	<i>RP11-402G3.3</i>
11	128238229	128238287	5	10.94	92.52	-81.58	11q24.3	0	<i>RP11-702B10.1</i>
2	175513074	175513181	4	11.46	93.19	-81.73	<b>2q31.1*</b>	58,435	<i>AC096649.3</i>
8	125656813	125661153	5	11.33	93.41	-82.07	8q24.13	87,902	<i>RP11-697B24.1</i>
X	17787319	17787370	4	11.39	93.77	-82.38	Xp22.13	12,679	<i>RAI2</i>
2	105469919	105470078	6	10.27	92.8	-82.53	<b>2q12.2*</b>	-31,407	<b>FHL2</b> ↓
4	81549092	81549168	5	12.58	95.15	-82.57	<b>4q21.22*</b>	0	<i>RASGEF1B</i>
10	12834415	12834475	5	11.88	94.62	-82.73	10p13	0	<b>CAMK1D</b> ↓
8	6206361	6206512	5	9.25	92.33	-83.09	8p23.2	0	<i>RP11-124B13.1</i>
21	42592315	42592389	4	9.08	92.41	-83.33	21q22.3	6,891	<i>AP001626.1</i>
1	77965941	77966010	6	7.78	91.37	-83.58	1p31.1	0	<i>FUBP1</i>
13	99372836	99372910	7	11.43	95.58	-84.15	<b>13q32.3†</b>	0	<i>UBAC2</i>
21	34187699	34187759	4	10.47	94.69	-84.22	21q22.11	0	<i>AP000320.7</i>
16	16366970	16367047	8	10.38	95.25	-84.87	16p13.11	0	<i>RP11-958N24.2</i>
7	46039538	46039742	7	9.08	94.07	-84.99	7p12.3	38,641	<i>AC073115.7</i>
6	127739572	127739639	6	10	95.25	-85.26	6q22.33	0	<b>THEMIS</b> ↓
5	7475707	7475827	4	10.82	96.43	-85.6	<b>5p15.31*</b>	0	<i>ADCY2</i>
12	102162366	102162539	4	7.88	93.85	-85.97	12q23.2	0	<i>PARBP</i>
19	38131299	38131450	4	9.2	95.29	-86.09	19q13.13	0	<i>SIPA1L3</i>
6	106228329	106228402	6	8.49	95.14	-86.65	6q21	0	<i>ATG5</i>

Genes differentially expressed in KTCN are marked in bold, and the direction of expression change (up or down) is indicated by an arrow. Diff methylation (%) is a difference between mean region methylation in KTCN and non-KTCN samples.

\* Regions overlapping KTCN linkage loci.

† Regions overlapping KTCN chromosome arms.

In summary, we presented herein the results of data analysis from the first study of DNA methylation changes in human KTCN corneas compared to non-KTCN samples. We were able to identify genomic regions with distinct patterns of DNA hypo- and hypermethylation and link them to previously found

KTCN susceptibility loci as well as transcriptomic disruption of Wnt signaling pathway observed in KTCN. These findings provide novel insights into the KTCN etiology, allowing us to elucidate some of the common mechanisms behind the development of this complex and heterogenic disease.

## Acknowledgments

Supported by National Science Centre in Poland, Grant 2012/05/E/NZ5/02127 (to MG).

Disclosure: **M. Kabza**, None; **J.A. Karolak**, None; **M. Rydzanicz**, None; **M. Udziela**, None; **P. Gasperowicz**, None; **R. Ploski**, None; **J.P. Szaflik**, None; **M. Gajecka**, None

## References

- Rabinowitz YS. Keratoconus. *Surv Ophthalmol*. 1998;42:297-319.
- Godefrooij DA, de Wit GA, Uiterwaal CS, Imhof SM, Wisse RPL. Age-specific incidence and prevalence of keratoconus: a nationwide registration study. *Am J Ophthalmol*. 2017;175:169-175.
- Abu-Amero KK, Al-Muammar AM, Kondkar AA. Genetics of keratoconus: where do we stand? *J Ophthalmol*. 2014;2014:641708.
- Nowak DM, Gajecka M. The genetics of keratoconus. *Middle East Afr J Ophthalmol*. 2011;18:2-6.
- Karolak JA, Gajecka M. Genomic strategies to understand causes of keratoconus. *Mol Genet Genomics*. 2017;292:251-269.
- Petronis A. Epigenetics as a unifying principle in the aetiology of complex traits and diseases. *Nature*. 2010;465:721-727.
- Trerotola M, Relli V, Simeone P, Alberti S. Epigenetic inheritance and the missing heritability. *Hum Genomics*. 2015;9:17.
- Matthews FJ, Cook SD, Majid MA, Dick AD, Smith VA. Changes in the balance of the tissue inhibitor of matrix metalloproteinases (TIMPs)-1 and -3 may promote keratocyte apoptosis in keratoconus. *Exp Eye Res*. 2007;84:1125-1134.
- De Bonis P, Laborante A, Pizzicoli C, et al. Mutational screening of VSX1, SPARC, SOD1, LOX, and TIMP3 in keratoconus. *Mol Vis*. 2011;17:2482-2494.
- Meissner A, Gnirke A, Bell GW, Ramsahoye B, Lander ES, Jaenisch R. Reduced representation bisulfite sequencing for comparative high-resolution DNA methylation analysis. *Nucleic Acids Res*. 2005;33:5868-5877.
- Kabza M, Karolak JA, Rydzanicz M, et al. Collagen synthesis disruption and downregulation of core elements of TGF- $\beta$ , Hippo, and Wnt pathways in keratoconus corneas. *Eur J Hum Genet*. 2017;25:582-590.
- Karolak JA, Gambin T, Rydzanicz M, et al. Evidence against ZNF469 being causative for keratoconus in Polish patients. *Acta Ophthalmol*. 2016;94:289-294.
- Krueger F, Andrews SR. Bismark: a flexible aligner and methylation caller for Bisulfite-Seq applications. *Bioinformatics*. 2011;27:1571-1572.
- Akalin A, Kormaksson M, Li S, et al. methylKit: a comprehensive R package for the analysis of genome-wide DNA methylation profiles. *Genome Biol*. 2012;13:R87.
- Park Y, Wu H. Differential methylation analysis for BS-seq data under general experimental design. *Bioinformatics*. 2016;32:1446-1453.
- Quinlan AR, Hall IM. BEDTools: a flexible suite of utilities for comparing genomic features. *Bioinformatics*. 2010;26:841-842.
- Gel B, Serra E. karyoploteR: an R/Bioconductor package to plot customizable genomes displaying arbitrary data. *Bioinformatics*. 2017;33:3088-3090.
- Hahne F, Ivanek R. Visualizing genomic data using gviz and bioconductor. In: *Statistical Genomics. Methods in Molecular Biology*. New York, NY: Humana Press; 2016:335-351.
- Yu G, Wang L-G, He Q-Y. ChIPseeker: an R/Bioconductor package for ChIP peak annotation, comparison and visualization. *Bioinformatics*. 2015;31:2382-2383.
- Patro R, Duggal G, Love MI, Irizarry RA, Kingsford C. Salmon provides fast and bias-aware quantification of transcript expression. *Nat Methods*. 2017;14:417-419.
- Law CW, Alhamdoosh M, Su S, Smyth GK, Ritchie ME. RNA-seq analysis is easy as 1-2-3 with limma, Glimma and edgeR. *F1000Res*. 2016;5:1408.
- Ritchie ME, Phipson B, Wu D, et al. Limma powers differential expression analyses for RNA-sequencing and microarray studies. *Nucleic Acids Res*. 2015;43:e47.
- Brancati F, Valente EM, Sarkozy A, et al. A locus for autosomal dominant keratoconus maps to human chromosome 3p14-q13. *J Med Genet*. 2004;41:188-192.
- Rosenfeld JA, Drautz JM, Clericuzio CL, et al. Deletions and duplications of developmental pathway genes in 5q31 contribute to abnormal phenotypes. *Am J Med Genet A*. 2011;155A:1906-1916.
- Gajecka M, Radhakrishna U, Winters D, et al. Localization of a gene for keratoconus to a 5.6-Mb interval on 13q32. *Invest Ophthalmol Vis Sci*. 2009;50:1531-1539.
- Hughes AE, Dash DP, Jackson AJ, Frazer DG, Silvestri G. Familial keratoconus with cataract: linkage to the long arm of chromosome 15 and exclusion of candidate genes. *Invest Ophthalmol Vis Sci*. 2003;44:5063-5066.
- Nowak DM, Karolak JA, Kubiak J, et al. Substitution at IL1RN and deletion at SLC4A11 segregating with phenotype in familial keratoconus. *Invest Ophthalmol Vis Sci*. 2013;54:2207-2215.
- Li X, Rabinowitz YS, Tang YG, et al. Two-stage genome-wide linkage scan in keratoconus sib pair families. *Invest Ophthalmol Vis Sci*. 2006;47:3791-3795.
- Burdon KP, Macgregor S, Bykhovskaya Y, et al. Association of polymorphisms in the hepatocyte growth factor gene promoter with keratoconus. *Invest Ophthalmol Vis Sci*. 2011;52:8514-8519.
- Li X, Bykhovskaya Y, Haritunians T, et al. A genome-wide association study identifies a potential novel gene locus for keratoconus, one of the commonest causes for corneal transplantation in developed countries. *Hum Mol Genet*. 2012;21:421-429.
- Bykhovskaya Y, Li X, Epifantseva I, et al. Variation in the lysyl oxidase (LOX) gene is associated with keratoconus in family-based and case-control studies. *Invest Ophthalmol Vis Sci*. 2012;53:4152-4157.
- Lu Y, Vitart V, Burdon KP, et al. Genome-wide association analyses identify multiple loci associated with central corneal thickness and keratoconus. *Nat Genet*. 2013;45:155-163.
- Sahebjada S, Schache M, Richardson AJ, et al. Evaluating the association between keratoconus and the corneal thickness genes in an independent Australian population. *Invest Ophthalmol Vis Sci*. 2013;54:8224-8228.
- Sahebjada S, Schache M, Richardson AJ, Snibson G, Daniell M, Baird PN. Association of the hepatocyte growth factor gene with keratoconus in an Australian population. *PLoS One*. 2014;9:e84067.
- Bae HA, Mills RAD, Lindsay RG, et al. Replication and meta-analysis of candidate loci identified variation at RAB3GAP1 associated with keratoconus. *Invest Ophthalmol Vis Sci*. 2013;54:5132-5135.
- Nakatsu MN, Ding Z, Ng MY, Truong TT, Yu F, Deng SX. Wnt/ $\beta$ -catenin signaling regulates proliferation of human cornea epithelial stem/progenitor cells. *Invest Ophthalmol Vis Sci*. 2011;52:4734-4741.
- Aldave AJ, Bourla N, Yellore VS, et al. Keratoconus is not associated with mutations in COL8A1 and COL8A2. *Cornea*. 2007;26:963-965.



38. Lev Maor G, Yearim A, Ast G. The alternative role of DNA methylation in splicing regulation. *Trends Genet.* 2015;31:274-280.
39. Galvis V, Sherwin T, Tello A, Merayo J, Barrera R, Acera A. Keratoconus: an inflammatory disorder? *Eye (Lond).* 2015;29:843-859.
40. Gasche JA, Hoffmann J, Boland CR, Goel A. Interleukin-6 promotes tumorigenesis by altering DNA methylation in oral cancer cells. *Int J Cancer.* 2011;129:1053-1063.
41. Morisawa S, Yasuda H, Kamiya T, Hara H, Adachi T. Tumor necrosis factor- $\alpha$  decreases EC-SOD expression through DNA methylation. *J Clin Biochem Nutr.* 2017;60:169-175.